

> REPLACE THIS LINE WITH YOUR MANUSCRIPT ID NUMBER (DOUBLE-CLICK HERE TO EDIT) <

This work has been submitted to the IEEE for possible publication. Copyright may be transferred without notice, after which this version may no longer be accessible.

Surpassing Cosine Similarity for Multidimensional Comparisons: Dimension Insensitive Euclidean Metric (DIEM)

Federico Tessari¹, Neville Hogan^{1,2}

Abstract—The advancement in computational power and hardware efficiency enabled the tackling of increasingly complex and high-dimensional problems. While artificial intelligence (AI) achieved remarkable results, the interpretability of high-dimensional solutions remains challenging. A critical issue is the comparison of multidimensional quantities, which is essential in techniques like Principal Component Analysis (PCA), or k-means clustering. Common metrics such as cosine similarity, Euclidean distance, and Manhattan distance are often used for such comparisons – for example in muscular synergies of the human motor control system. However, their applicability and interpretability diminish as dimensionality increases. This paper provides a comprehensive analysis of the effects of dimensionality on these metrics. Our results reveal significant limitations of cosine similarity, particularly its dependency on the dimensionality of the vectors, leading to biased and less interpretable outcomes. To address this, we introduce the Dimension Insensitive Euclidean Metric (DIEM) which demonstrates superior robustness and generalizability across dimensions. DIEM maintains consistent variability and eliminates the biases observed in traditional metrics, making it a reliable tool for high-dimensional comparisons. This novel metric has the potential to replace cosine similarity, providing a more accurate and insightful method to analyze multidimensional data in fields ranging from neuromotor control to machine and deep learning.

Index Terms — Cosine Similarity, Distance Measurement, Dimensionality Reduction, Euclidean Distance, Information Retrieval

I. INTRODUCTION

THE continuous growth of computational capabilities combined with the improvement of hardware efficiency [1] granted the possibility to approach problems of growing complexity and dimensionality. Over a little more than two decades, Artificial intelligence (AI) agents were able to defeat humans in games considered – up to that point – dominated by humans: chess [2], Go [3], Starcraft II [4]. This capability to handle very complex and highly dimensional problems also led to promising results in different fields such as molecular biology [5] or robotics [6]. On one hand, the results of these computing techniques are undeniably

impressive; on the other hand, their interpretability appears to decrease with their complexity and dimensionality.

Among the difficulties in the interpretation of these tools, a concern is the comparison of multidimensional quantities. For example, in dimensionality reduction techniques, such as Principal Component Analysis (PCA), Singular Value Decomposition (SVD), or k-means clustering, the algorithms extract significant combinations of a selected set of input features. The number of input features can vary greatly, from tens – for example when considering the joint angles of the hand [7] – to hundreds such as when looking at high density electromyograms. A reasonable question that arises from this extraction process is: “How similar or different are these combinations of features from different data sources e.g., subjects, experiments, or iterations?”

Two practical examples might provide a better understanding. Consider, for instance, the task of identifying the individual user-preferences for movies based on a series of input features such as the movies the user has watched, his/her evaluation of the movies, and the date when they were watched [8]. Alternatively, consider the task of identifying during a given motor task e.g., grasping an object, how a certain individual coordinates his/her different joints (shoulder, elbow, wrist, phalanges) to successfully complete that motor action [9], [10]. Assuming the algorithm identifies specific individuals’ preferences based on those given input features, how can we compare two different individuals’ preferences? Answering this question is interesting because it can provide insight on the individuals’ decision making-processes (movie example) or underlying control strategies (motor control example).

As long as the number of input features is limited to 2 or 3, humans are visually able to interpret them using a planar or spatial analogy. However, when feature spaces go beyond 3D, visualization and interpretation become more complex and less intuitive. As a consequence, researchers typically rely on mathematical measurements that provide an alternative understanding of the similarity (or difference) between n -dimensional quantities.

Among the most widely adopted methods for multidimensional comparisons, cosine similarity stands as one

This work was supported by the Eric P. and Evelyn Newman Fund.

Corresponding Author: Federico Tessari, ftessari@mit.edu.

Federico Tessari is with Department of Mechanical Engineering, Massachusetts Institute of Technology, Cambridge, 02139, USA, (e-mail: ftessari@mit.edu).

Neville Hogan is with Department of Mechanical Engineering as well as the Department of Brain and Cognitive Sciences, Massachusetts Institute of Technology, Cambridge, 02139, USA (e-mail: neville@mit.edu).

Appendix is included after the main manuscript.

Color versions of one or more of the figures in this article are available online at <http://ieeexplore.ieee.org>

> REPLACE THIS LINE WITH YOUR MANUSCRIPT ID NUMBER (DOUBLE-CLICK HERE TO EDIT) <

of the gold standards [11], [12], [13], [14], [15], [16]. The main reasons behind its use are likely related to its analogy with angular measurements and its bounded and well-defined range (between 0 and 1, or -1 and 1, depending on which formulation is used). Alternatives to cosine similarity have been proposed using, for example: (i) inner-products approximations [17], (ii) ‘norms’ or distance metrics, such as the Manhattan distance (1-norm) or the Euclidean distance (2-norm), (iii) or combinations of existing methods [18]. Interestingly, the interpretation of these comparison metrics is often limited to lower dimensional cases (2D or 3D), and it is typically extrapolated to higher dimensional cases without much justification.

In this work, we present a detailed analysis of the effects of dimensionality on three of the most common metrics for multidimensional comparison: cosine similarity, Euclidean distance and Manhattan distance. From the analysis of these metrics, some interesting limitations and properties emerge, leading to the conclusion that the use of cosine similarity might not be the most appropriate choice for multidimensional comparisons. An alternative to these three metrics, derived from the Euclidean distance, is proposed which shows better robustness and generalizability to increasing number of dimensions. The new metric – named DIEM (Dimension Insensitive Euclidean Metric) – is a candidate to surpass and replace the use of cosine similarity for high dimensional comparisons.

II. COSINE SIMILARITY AND EUCLIDEAN DISTANCE

Given two vectors $\mathbf{a} = [a_1 \dots a_n]$ and $\mathbf{b} = [b_1 \dots b_n]$, with $a_i, b_i \in \mathbb{R}$; the cosine similarity between these vectors is defined as:

$$\cos(\theta) = \frac{|\mathbf{a}^T \cdot \mathbf{b}|}{\|\mathbf{a}\| \cdot \|\mathbf{b}\|} \quad (1)$$

This value ranges between 0 and 1, with 0 meaning the two vectors are orthogonal, and 1 meaning the vectors are collinear. This measure is often used in the study of kinematic and muscle synergies (identified via principal components) to estimate the degree of similarity between such principal components. This is done because each principal component can be considered a direction in the hyperspace that contains it.

A. Relation to Euclidean Distance

We can consider the \mathbf{a} and \mathbf{b} vectors as points in the n -dimensional space, and we can compute the Euclidean distance i.e., 2-norm, between them as:

$$d = \sqrt{\sum_{i=1}^n (a_i - b_i)^2} \quad (2)$$

This relation can be reworked to obtain:

$$\begin{aligned} d &= \sqrt{\sum_{i=1}^n (a_i - b_i)^2} = \sqrt{\sum_{i=1}^n (a_i^2 - 2a_i b_i + b_i^2)} \Rightarrow d^2 \\ &= \sum_{i=1}^n (a_i^2 - 2a_i b_i + b_i^2) \Rightarrow \\ d^2 &= \sum_{i=1}^n a_i^2 + \sum_{i=1}^n b_i^2 - 2 \sum_{i=1}^n a_i b_i \quad (3) \end{aligned}$$

We can then reformulate Eq. 1 in index notation:

$$\cos(\theta) = \frac{|\mathbf{a}^T \cdot \mathbf{b}|}{\|\mathbf{a}\| \cdot \|\mathbf{b}\|} = \frac{|\sum_{i=1}^n a_i b_i|}{\|\mathbf{a}\| \cdot \|\mathbf{b}\|} \quad (4)$$

Remembering that the Euclidean norm of a vector is equal to $\|\mathbf{x}\| = \sqrt{\sum_{i=1}^n x_i^2}$, and combining Equation 4 and Equation 3, we obtain:

$$\cos(\theta) = \frac{1}{\|\mathbf{a}\| \cdot \|\mathbf{b}\|} \cdot \left| \frac{\|\mathbf{a}\|^2 + \|\mathbf{b}\|^2 - d^2}{2} \right| \quad (5)$$

Equation (5) shows that the cosine similarity has a quadratic correlation with the Euclidean distance. Moreover, in the case in which our vectors \mathbf{a}, \mathbf{b} present unit length, this relation simplifies to:

$$\cos(\theta) = \left| 1 - \frac{d^2}{2} \right| \quad (6)$$

For unit-length vectors, the Euclidean distance can only range between $0 \leq d \leq 2$, since the vectors – independently of the dimension of space that they span – could at most be on a diameter of a hyper-sphere of radius 1. Figure 1 provides a graphical representation of Equation (6).

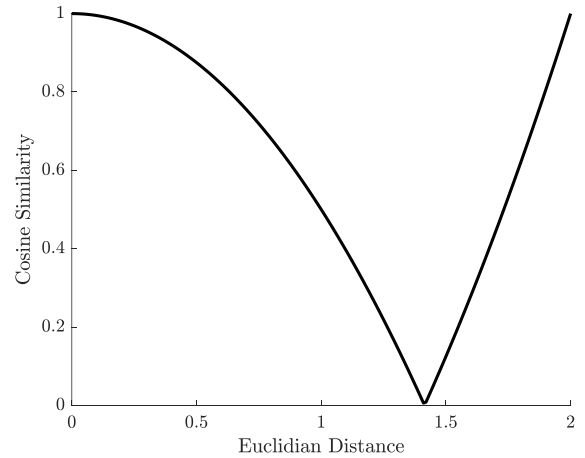


Fig. 1. Graphical representation of the relation between cosine similarity and Euclidean distance for unit length vectors.

Equation 6 can also be derived using Pythagoras’ theorem on the red triangle highlighted in Figure 2.

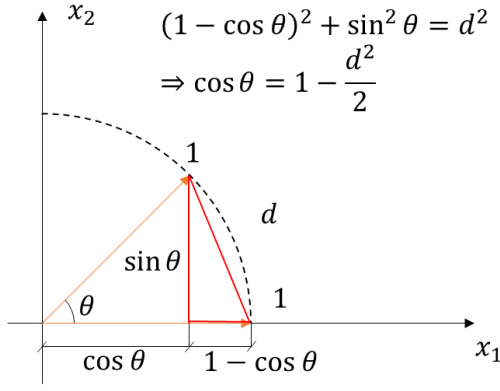


Fig. 2. Geometrical relation between the angle spanned by two unit vectors and the Euclidean distance between their end points.

III. EFFECT OF THE VECTORS' DIMENSIONALITY

A second interesting aspect is the sensitivity of the cosine similarity metric to the dimension of the considered vectors (n) as well as to the space spanned by them: \mathbb{R}^n , \mathbb{R}^{n+} , \mathbb{R}^{n-} .

In order to test the sensitivity to these two aspects, a numerical simulation was run using the algorithm presented in Figure 3. The idea was to iterate through growing dimensions while comparing two randomly generated vectors (\mathbf{a} , \mathbf{b}).

The vectors were generated from a pseudo-uniform distribution in order to avoid bias on the mean value of each vector's elements. The cosine similarity was computed for a range of dimensions going from 2 (planar case) to 102.

Vectors \mathbf{a} , \mathbf{b} were scaled such that, in the three different domains, their lengths assumed the following range of values: $\mathbb{R} \rightarrow -1 \leq a_i, b_i \leq 1 \forall i$, $\mathbb{R}^+ \rightarrow 0 \leq a_i, b_i \leq 1 \forall i$, $\mathbb{R}^- \rightarrow -1 \leq a_i, b_i \leq 0 \forall i$. Figure 4 shows three randomly generated vectors of dimension $n = 12$ for the three aforementioned ranges.

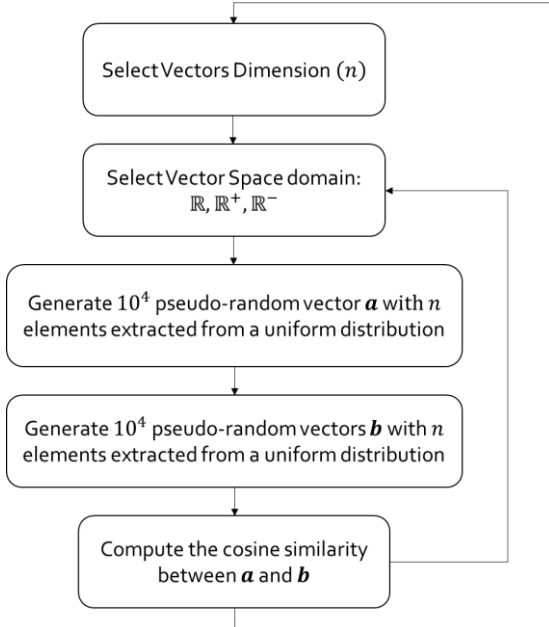


Fig. 3. Algorithm used for the sensitivity analysis of the cosine similarity with respect to vectors' dimension and domain.

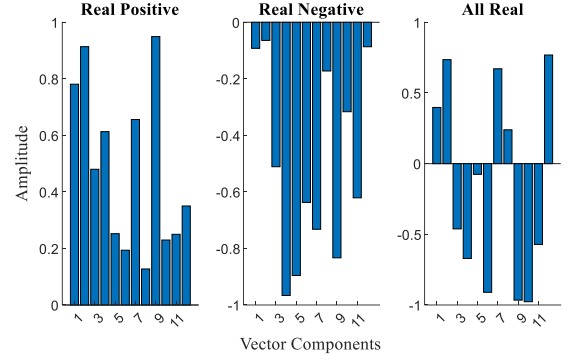


Fig. 4. Three randomly generated vectors from the real positive, real negative and all real domains. Each element was extracted from a pseudo-uniform distribution with preset ranges.

These ranges were arbitrarily chosen to resemble the activation level of some feature e.g., a surface electromyographic signal normalized to maximum voluntary activation. A sensitivity analysis of the vector scaling demonstrated that it produced no effect on cosine similarity. The resulting cosine similarities for each vector dimension and each vector domain are presented in Figure 5.

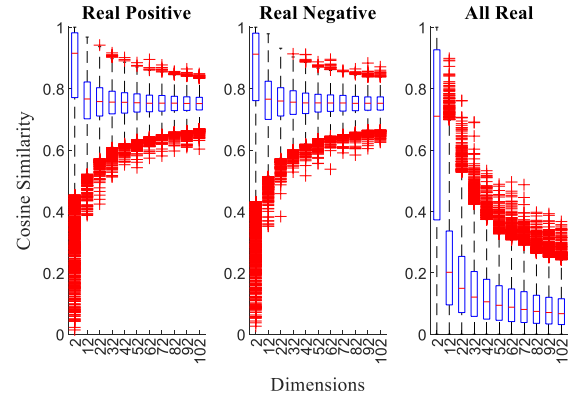


Fig. 5. Cosine similarity boxplots for increasing dimension of the vectors \mathbf{a} and \mathbf{b} . The three panels show, respectively, the case in which vectors elements were only positive (left), only negative (center) or could assume all real values within the given range (right).

Interestingly, the growing dimensionality of these random vectors led to a convergence of the average cosine similarity. For the only-positive or only-negative vectors, cosine similarity rapidly converged to a value of about 0.75 ± 0.1 . For the vectors that could span both negative and positive values, the cosine similarity converged to a value of less than 0.1.

This analysis has been replicated using, as comparison metric, the Euclidean distance between normalized vectors (Figure 6).

> REPLACE THIS LINE WITH YOUR MANUSCRIPT ID NUMBER (DOUBLE-CLICK HERE TO EDIT) <

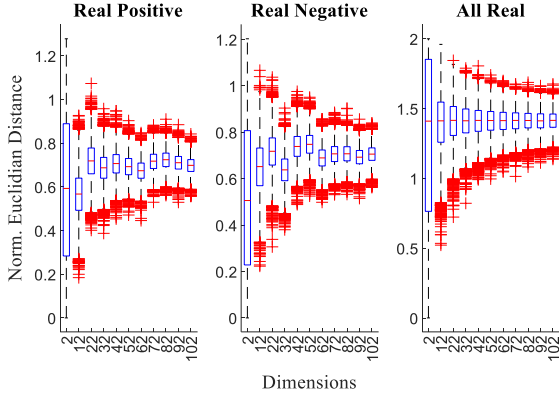


Fig. 6. Normalized Euclidean distance for increasing dimension of the vectors \mathbf{a} and \mathbf{b} . The three panels show, respectively, the case in which vectors elements were only positive (left), only negative (center) or could assume all real values within the given range (right).

Also in this case, the normalized Euclidean distance converged toward a constant value with limited variability. Specifically, for the real positive and negative cases the metric converged to about 0.7 ± 0.1 , while for the all-real case it converged to 1.41 ± 0.2 . This value is close to $\sqrt{2}$, which is the expected distance between two unit vectors perfectly orthogonal to each other. In fact, for the all-real case of Figure 5, we observed the cosine similarity converging towards zero i.e., the vectors approached orthogonality.

A more troubling aspect – emerging from both the cosine similarity and normalized Euclidean distance (Figures 5 and 6) – was the fact that the scatter i.e., variability, of these metrics was a strong function of the number of dimensions (n). Specifically, the variability of these random comparisons tended to narrow with the increase of number of dimensions.

Different distributions for sampling the vectors \mathbf{a}, \mathbf{b} , such as the Gaussian or uniform spherical distribution, were tested showing equivalent results to what is presented in Figures 5 and 6. Please refer to the Appendix for further details. If, instead, we consider the non-normalized Euclidean distance, we observe the behavior presented in Figure 7.

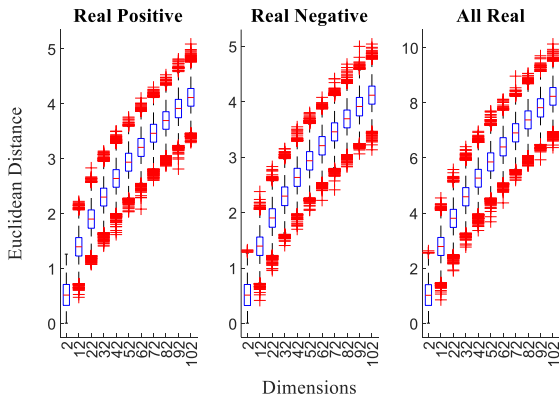


Fig. 7. Euclidean distance for increasing dimension of the vectors \mathbf{a} and \mathbf{b} . The three panels show, respectively, the case in which vectors elements were only positive (left), only negative (center) or could assume all real values within the given range (right).

The center of the Euclidean distance distribution tended to grow without bound, but the variability of each boxplot remained approximately constant. This is an improvement over the cosine similarity or normalized Euclidean distance case for two reasons: (i) the variability does not change with the dimension of the vectors \mathbf{a} and \mathbf{b} , (ii) the metric does not converge towards a plateau.

IV. MATHEMATICAL PROPERTIES OF THE EUCLIDEAN DISTANCE

Some interesting properties can be analytically derived from the definition of Euclidean distance (Equation 2), assuming that each element of any two vectors \mathbf{a}, \mathbf{b} is bounded between a minimum v_m and maximum value v_M , with $v_M > v_m$. This boundedness is a reasonable assumption, since measurable physical quantities are typically bounded either by physical or measurement limitations.

Considering these assumptions, the minimum Euclidean distance between any two n -dimensional vectors \mathbf{a} and \mathbf{b} is always zero independent of dimension:

$$d_{min}(n) = 0 \quad \forall n \quad (7)$$

This is trivially demonstrated by assuming that:

$$\forall i = 1, \dots, n \rightarrow a_i = b_i \quad (8)$$

The maximum Euclidean distance can be computed considering that – for a given dimension n – each element of the vector \mathbf{a} assumes its maximum value v_M , while each element of the other vector \mathbf{b} assumes its minimum value v_m . At that point, the Euclidean distance of Equation 2 becomes:

$$d = \sqrt{\sum_{i=1}^n (a_i - b_i)^2} \leq \sqrt{\sum_{i=1}^n (v_M - v_m)^2} = \sqrt{n(v_M - v_m)^2}$$

$$\Rightarrow d_{max}(n) = \sqrt{n} \cdot (v_M - v_m) \quad (9)$$

Moreover, assuming the elements of the two vectors (\mathbf{a}, \mathbf{b}) are sampled from two independent and identically distributed (i.i.d.) random variables with uniform distributions: $a_i \sim U(v_m, v_M), b_i \sim U(v_m, v_M)$; it is possible to analytically derive the upper bound of the expected Euclidean distance i.e., the main trend observed in Figure 7. Specifically, by applying the Jensen’s inequality¹ [19] and the “Law Of The Unconscious Statistician” (LOTUS) [20] we obtain:

¹ The Jensen’s Inequality assumes concavity, and the square root function is indeed concave. This allows for the first ‘less-than-or-equal’ in Equation 10.

> REPLACE THIS LINE WITH YOUR MANUSCRIPT ID NUMBER (DOUBLE-CLICK HERE TO EDIT) <

$$\begin{aligned}
 E[d] &= E \left[\sqrt{\sum_{i=1}^n (a_i - b_i)^2} \right] \leq \sqrt{E \left[\sum_{i=1}^n (a_i - b_i)^2 \right]} \\
 &= \sqrt{n \cdot E[(a - b)^2]} \\
 &= \sqrt{n} \left(\iint_{v_m v_m}^{v_M v_M} \frac{(a - b)^2}{(v_M - v_m)^2} da db \right)^{\frac{1}{2}} \quad (10)
 \end{aligned}$$

The integral in Equation 10 can easily be solved by direct integration. We leave readers the pleasure to do so. The final results can be expressed in the following form:

$$\begin{aligned}
 E[d] &\leq \sqrt{n} \sqrt{\frac{2}{3}(v_M^2 + v_M v_m + v_m^2) - \frac{1}{2}(v_M + v_m)^2} \\
 &= \sqrt{\frac{n}{6}}(v_M - v_m) \quad (11)
 \end{aligned}$$

Equation 11 provides an analytical upper bound to the expected Euclidean distance between any two random vectors $\mathbf{a}, \mathbf{b} \sim U(v_m, v_M)$. Figure 8 provides a graphical representation of the Euclidean distance with also its maximum (Equation 9), minimum (Equation 7), and expected (Equation 11) value across dimensions.

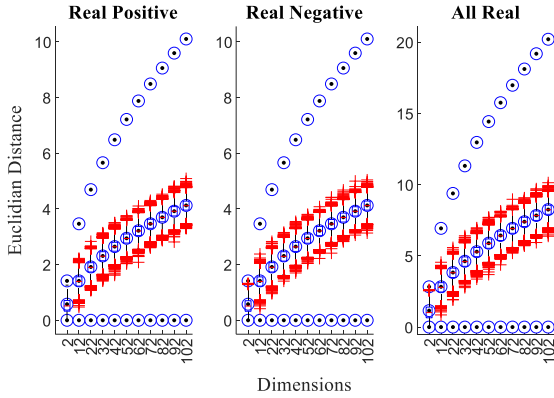


Fig. 8. Euclidean distance for increasing dimensions of the vectors \mathbf{a} and \mathbf{b} . The three panels show, respectively, the case in which vector elements were only positive (left), only negative (center) or could assume all real values within the given range (right). The blue circles show the minimum, maximum and expected analytical Euclidean distance values.

Interestingly, the obtained expected Euclidean distance upper bound is practically indistinguishable from the median value of the boxplots obtained through numerical simulation for any dimension $n > 2$. Moreover, it is also interesting to observe that the expected value is smaller than the arithmetic mean between the maximum and minimum Euclidean distance:

$$\begin{aligned}
 \frac{d_{min}(n) + d_{max}(n)}{2} &= \frac{\sqrt{n}}{2}(v_M - v_m) \Rightarrow \\
 \frac{\sqrt{n}}{2}(v_M - v_m) &> \sqrt{\frac{n}{6}}(v_M - v_m) \quad (12)
 \end{aligned}$$

Another interesting aspect to observe is the evolution of the Euclidean distance distribution for growing dimensions. The Real

Positive case was considered, but equivalent results were obtained for Real Negative and All Real cases.

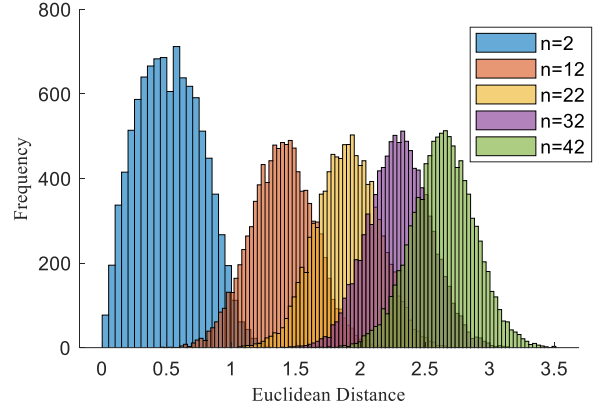


Fig. 9. Histograms of the non-normalized Euclidean distance for growing dimensions ‘n’.

For each of the simulated dimensions (n), a Kolmogorov-Smirnov test was performed to check whether the observed simulated distribution was significantly different from a normal distribution with mean and standard deviation equal to those of the simulated data $N(\text{mean}(d), \text{std}(d))$. Interestingly, the test showed a significant difference only for $n = 2$ ($p < 0.05$); while, for all the other tested dimensions the distribution of Euclidean distances was not significantly different from a normal distribution. A finer simulation on a subset of dimensions ($2 \leq n \leq 12$) revealed a smooth transition between non-normal and normal distribution around $n \cong 7$. Please refer to the Appendix for a detailed presentation of the transition between non-normal and normal distributions.

A confirmation of these results can be found in the work of Thirey and Hickam [21] in which they analytically derived the distribution of Euclidean distances between randomly distributed Gaussian vectors and observed a normalization of the distribution with increasing number of dimensions n .

Despite this normalization trend of the distribution of Euclidean distances, it is important to underline that the distribution tails are not symmetric. This is clearly observable from Figure 8 and it finds demonstration in Equation 12, since the expected value $E[d]$ is smaller than the mean between the maximum and minimum Euclidean distance. This asymmetry suggests that the distribution of Euclidean distance is not properly normal though it is effectively indistinguishable from normal.

V. A DIMENSION-INSENSITIVE METRIC FOR MULTIDIMENSIONAL COMPARISONS

At this point, we can obtain a dimension-insensitive metric by subtracting from each Euclidean distance distribution its expected value ($E[d(n)]$) i.e., the main trend, normalize it by the variance ($\sigma(n)^2$) at a dimension of interest and scale it to the range of the analyzed quantities ($v_M - v_m$). The resulting metric has been named ‘Dimension Insensitive Euclidean Metric’ (DIEM):

> REPLACE THIS LINE WITH YOUR MANUSCRIPT ID NUMBER (DOUBLE-CLICK HERE TO EDIT) <

$$DIEM = \frac{v_M - v_m}{\sigma(n)^2} \left(\sqrt{\sum_{i=1}^n (a_i - b_i)^2} - E[d(n)] \right) \quad (13)$$

The resulting distributions for the DIEM are presented in Figure 10.

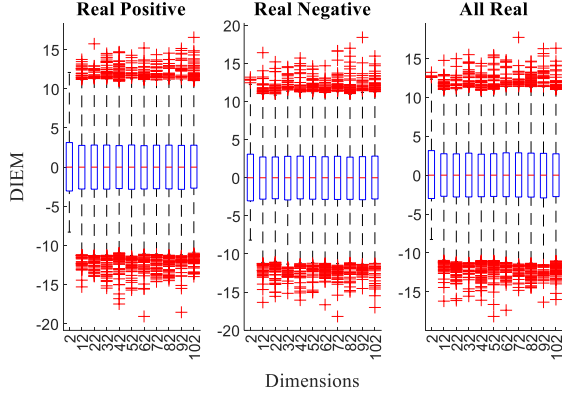


Fig. 10. Dimension Invariant Euclidean Metric (DIEM) for increasing dimension of the vectors \mathbf{a} and \mathbf{b} . The three panels show, respectively, the case in which vector elements were only positive (left), only negative (center) or could assume all real values within the given range (right).

Figure 10 shows that increasing the number of dimensions does not affect either the converged value nor the variance of the measurements, thus providing a more reliable comparison metric for high-dimensional vectors. Moreover, the histograms of Dimension Invariant Euclidean Metric show how the distributions are practically identical for $n \geq 7$ (Figure 11).

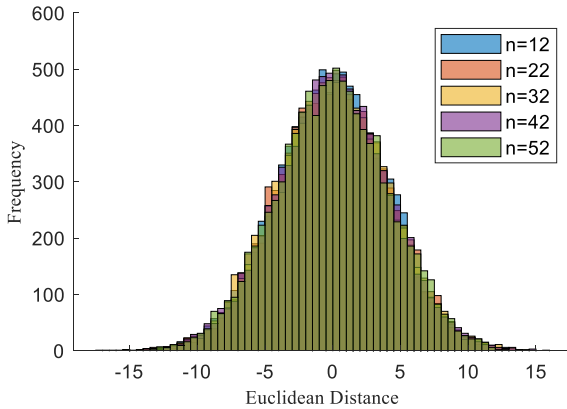


Fig. 11. Histograms of the detrended Euclidean distance for growing dimensions 'n'.

A more intuitive understanding of similarity and dissimilarity using DIEM is provided in Figure 12. In general, vectors may have different magnitudes and orientations. Lower values of DIEM represent similar vectors, while higher values of the metric represent dissimilar vectors. Since the DIEM is detrended, its expected value $E[DIEM]$ is 0. The shaded red areas respectively show one, two and three standard deviations

(σ). Three dotted lines are added to present, respectively, the maximum Dimension Invariant Euclidean Metric ($DIEM_{max}$) – which represents antiparallel vectors with maximum magnitude, the average Dimension Invariant Euclidean Metric between orthogonal vectors ($E[DIEM_{orth}]$) and the minimum Dimension Invariant Euclidean Metric ($DIEM_{min}$) – which represents identical vectors.

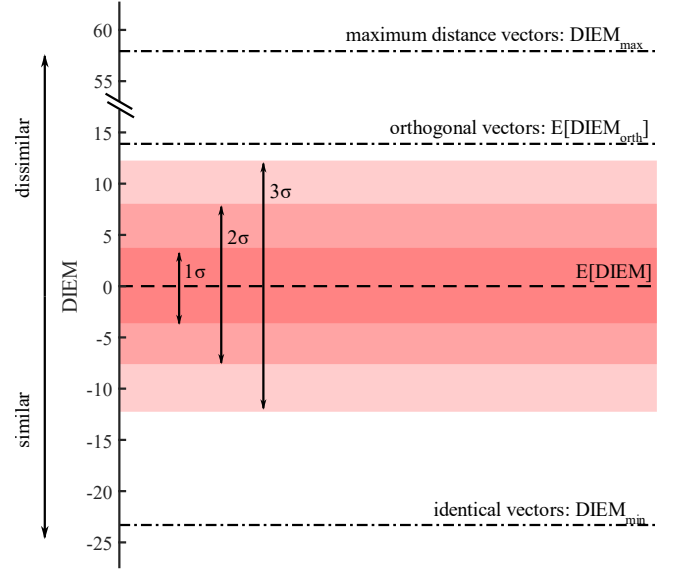


Fig. 12. Explanatory scheme of the Dimension Invariant Euclidean Metric (DIEM). This image was generated considering $n = 12, v_M = 1, v_m = 0, \sigma(12)^2 = 16.74$. The dashed black line represents the expected DIEM. The red colored bands represent respectively one, two and three standard deviations of the DIEM distribution. The top dotted black line is the maximum $DIEM_{max} = 57.98$, representing two opposing vectors with maximum magnitude. The second from top dotted black line is the median value of the DIEM for orthogonal vectors $E[DIEM_{orth}] = 13.95$. The bottom dotted black line is the minimum $DIEM_{min} = -23.34$, representing two identical vectors.

The median Dimension Invariant Euclidean Metric between orthogonal vectors ($E[DIEM_{orth}]$) was computed by generating a series of orthogonal vectors and numerically computing their expected value. From the considered case in Figure 12 ($n = 12, v_M = 1, v_m = 0, \sigma(12)^2 = 16.74$), the probability of two random vectors to be orthogonal was more than three standard deviations from the mean.

The minimum DIEM is easily obtained combining Equation (7) with Equation (13):

$$DIEM_{min} = - \frac{v_M - v_m}{\sigma(n)^2} E[d(n)] \quad (14)$$

while maximum DIEM is obtained considering Equation (9) in combination with Equation (13):

$$DIEM_{max} = \frac{v_M - v_m}{\sigma(n)^2} (\sqrt{n} \cdot (v_M - v_m) - E[d(n)]) \quad (15)$$

It is worth emphasizing that, while the expected value of the Dimension Invariant Euclidean Metric ($E[DIEM]$) as well as its variance (and standard deviation) remain constant

independent of the number of dimensions, the value of the maximum and minimum Dimension Insensitive Euclidean Metric ($DIEM_{max}, DIEM_{min}$) as well as the expected distance between orthogonal vectors ($E[DIEM_{orth}]$) are functions of $E[d(n)]$ and, thus, of the number of dimensions. Both quantities are, however, numerically computable either by numerical simulation ($E[DIEM_{orth}]$) or by direct derivation ($DIEM_{max}, DIEM_{min}$).

An interesting question is whether the mathematical properties of the Euclidean distance are unique to the 2-norm or generalize to different norms. In this context, another common metric for comparison of multi-dimensional vectors is the Manhattan distance or 1-norm. Considering two vectors \mathbf{a}, \mathbf{b} , each composed by n elements; the Manhattan distance is defined as:

$$d_M = \sum_{i=1}^n |a_i - b_i| \quad (15)$$

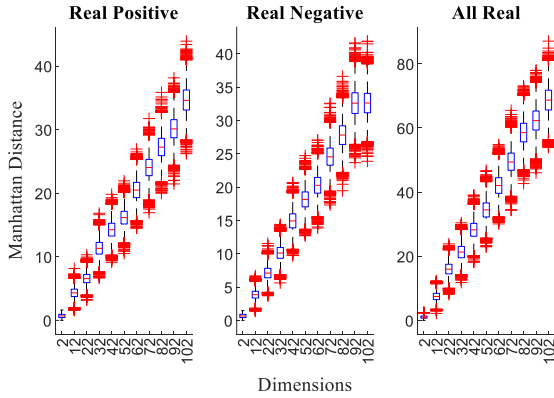


Fig. 13. Manhattan distance for increasing dimension of the vectors \mathbf{a} and \mathbf{b} . The three panels show, respectively, the case in which vectors elements were only positive (left), only negative (center) or could assume all real values within the given range (right).

Applying the same algorithm presented in Figure 3, Figure 13 presents the Manhattan distance evolution with increasing dimensions (n). The Manhattan distance grows linearly with respect to the number of dimensions, and this can be demonstrated by calculating the maximum Manhattan distance value between two random vectors and realizing that it grows proportionally to n :

$$d_{M_{max}}(n) = n|v_{max} - v_{min}| \quad (16)$$

More interestingly, the variance of the Manhattan distance does not remain constant with the increase in dimensions as it does for the Euclidean distance. It actually grows with dimensions. This is a limitation of its applicability for a dimension-insensitive metric compared to the Euclidean metric presented in this work. Higher order norms e.g., 3-norm, 4-norm, and so on, could be attempted, but that investigation is not treated here.

VI. DISCUSSION

In the study of multidimensional quantities (e.g., principal components extracted through PCA), cosine similarity is used – independently of the dimension – as a metric to assess similarity between such quantities. Our results show that such a metric is strongly influenced by the dimension of the investigated vector. For example, if we look in Figure 5 at dimension $n = 2$ (planar case), we observe – in all three cases – that the cosine angle between two random vectors \mathbf{a} and \mathbf{b} led to a broad almost uniform distribution of cosine similarity between 0 and 1, as we might expect. However, as soon as we moved away from the planar case ($n = 2$), the distribution of cosine similarity narrowed and converged, thus limiting the interpretability of this metric. Purely random vectors yielded an apparent similarity of about 0.75. That implies an included angle of about 41 degrees, apparently closer to collinearity than orthogonality, based on chance alone.

A practical example can be derived from the study of muscle synergies. Let's imagine we extract muscle synergies using non-negative matrix factorization [22] from two different subjects performing the same task. We later want to compare the synergy composition that accounts for most of the variation between subjects. Such a synergy composition would typically look similar to what was presented in the left panel of Figure 4 i.e., an n -dimensional vector with n equal to the number of sampled muscles. The vector elements can assume only positive values, since post-processed muscular activity sampled through electromyography is typically rectified.

Now if n is greater than 2, as in many cases, our analysis in Figure 5 shows that any random vector extracted from the same distribution will tend to converge toward a similarity of 0.75 with a limited overall range. Therefore, if from our 2-synergy comparison we observe a similar value (say 0.75), we won't be able to determine whether such synergies are effectively similar to each other, or simply the result of a random chance. Similar considerations apply to synergies extracted from kinematic features, which are able to span the whole real range, thus following a behavior similar to the rightmost panel of Figure 5. This emphasizes the importance of considering the dimensionality of the considered vectors to correctly assess if the two vectors are effectively similar (collinear) or dissimilar (orthogonal).

Similar results are obtained when analyzing the normalized Euclidean distance, in agreement with Equation 6. However, if instead we consider the non-normalized Euclidean distance, we achieve two interesting results (refer to Figure 7): (i) the metric is unbounded; the center of its distribution increases with the square root of the number of dimensions, (ii) its variability appears to remain constant.

By detrending the Euclidean distance boxplots (Figure 10) – in our case using the expected value – we obtain a metric to measure the similarity or dissimilarity between hyper-dimensional vectors that is **insensitive** of the number of considered dimensions (n). This feature appears to be a particular property of the Euclidean distance. In fact, when using a different norm (Manhattan distance), the resulting behavior does not guarantee a dimension-insensitive variance (Figure 12). Moreover, for $n \geq 7$, the resulting distribution of detrended Euclidean distances is statistically indistinguishable

> REPLACE THIS LINE WITH YOUR MANUSCRIPT ID NUMBER (DOUBLE-CLICK HERE TO EDIT) <

from a normal distribution (Figure 11). This opens access to a very broad set of test methods for statistical comparisons e.g., t-tests or ANOVA.

The analysis and comparison of multi-dimensional quantities – such as synergies in the human neuromotor control literature or principal components and clusters in deep learning methods – has represented a thorny and often ‘neglected’ aspect. Most studies rely on comparison metrics e.g., the cosine similarity, without a complete understanding of their dependency on the number of dimensions of the considered features. Our study reveals that this dimensional dependency can significantly bias the interpretation of these metrics, leading to potentially erroneous conclusions. In response to this challenge, we introduce the Dimension Insensitive Euclidean Metric (DIEM), which effectively mitigates the dimensional dependency issue, providing a more accurate and interpretable measure for multi-dimensional comparisons. DIEM’s ability to maintain consistent variability across dimensions opens new avenues for robust statistical analysis and hypothesis testing, facilitating deeper insights into complex data structures. By adopting DIEM, researchers can enhance the reliability of their multi-dimensional analyses, paving the way for more precise and meaningful interpretations in fields ranging from neuromotor control to deep learning. Future research should continue to explore and refine this metric, ensuring its broad applicability and further validating its advantages over traditional methods.

APPENDIX

I. EFFECT OF VECTORS’ DISTRIBUTION

The effect of dimensionality on randomly generated vectors (\mathbf{a}, \mathbf{b}) was tested on elements drawn from three different distributions: (i) uniform (Figure 4), (ii) Gaussian (Figure S1), (iii) uniformly distributed on a unit sphere (Figure S2) [23], [24]. The same algorithm proposed in Figure 3 was adopted.

In the Gaussian distribution case, the elements of the vectors (\mathbf{a}, \mathbf{b}) were sampled from Gaussian distributions with mean and standard deviation respectively equal to: real positive $\mu = 0.5, \sigma = 0.3$, real negative $\mu = -0.5, \sigma = 0.3$, all real $\mu = 0, \sigma = 0.6$.

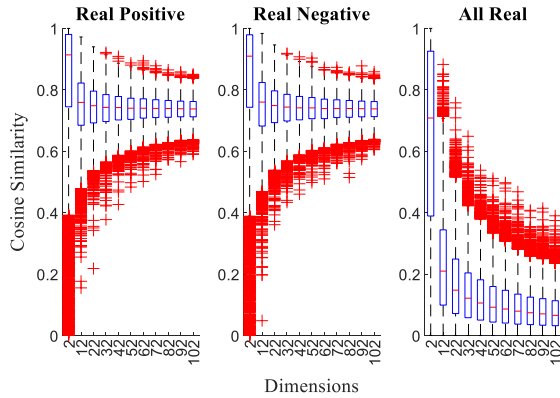


Fig. S1. Cosine similarity boxplots for increasing dimension of the vectors \mathbf{a} and \mathbf{b} . The three panels show, respectively, the case in which vector elements were only positive (left), only

negative (center) or could assume all real values within the given range (right). The elements of the vectors were sampled from a Gaussian distribution.

In the case of a uniform unit sphere distribution, the elements of the vectors (\mathbf{a}, \mathbf{b}) were sampled from a uniform distribution following the approach presented in the main manuscript (Section “Effects of Vector’ Dimensionality”) and then projected to a unit n-sphere following the algorithm presented in the works by Marsaglia and Muller [23], [24].

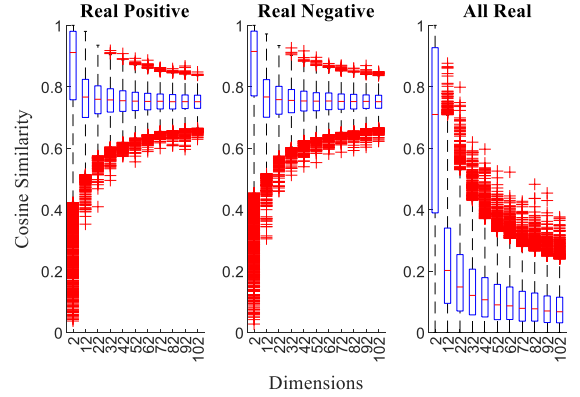


Fig. S2. Cosine similarity boxplots for increasing dimension of the vectors \mathbf{a} and \mathbf{b} . The three panels show, respectively, the case in which vectors elements were only positive (left), only negative (center) or could assume all real values within the given range (right). The elements of the vectors were sampled from a uniform unit n-sphere distribution.

Figure S1 and S2 align with the results presented in Figure 4, confirming that the cosine similarity metric shows a converging trend with decreasing variance for every tested distribution. The reason for this behavior can be attributed to the normalization of the vectors (\mathbf{a}, \mathbf{b}) in the mathematical formulation of the cosine similarity (Equation 1). This normalization causes the considered distributions to ‘collapse’ onto a unit n-dimensional sphere.

In the authors’ opinion, a uniform distribution is the most representative of a real scenario especially when the vectors represent physical quantities. For example, if the elements of the vectors \mathbf{a}, \mathbf{b} are physical quantities – such as force or position – acquired through sensors, they will arguably have the same probability to be sampled between the minimum ‘ v_m ’ and maximum ‘ v_M ’ of the sensor sampling range, thus justifying the uniform distribution. However, for completeness we explored distributions that might occur in different data processing conditions.

Figure S3 provides an intuitive bi-dimensional understanding of the difference between vectors (or points) sampled from the uniform, Gaussian and uniformly distributed unit sphere distributions. Despite these different distributions, Figures S1, S2 and Figure 4 show that the main trends used to define DIEM were observed in all cases.

> REPLACE THIS LINE WITH YOUR MANUSCRIPT ID NUMBER (DOUBLE-CLICK HERE TO EDIT) <

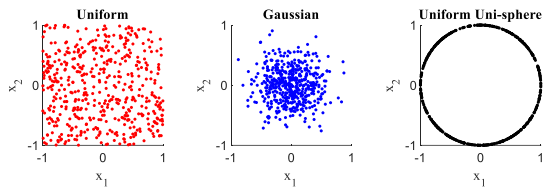


Fig. S3. Two dimensional points sampled with from three different distributions. The left plot (red dots) shows points sampled from a uniform distribution $U(-1,1)$. The central plot (blue dots) shows points sampled from a Gaussian distribution with mean 0 and standard deviation 0.3. The right plot (black dots) shows points sampled from a uniform distribution on the unit sphere ($r = 1$).

II. TRANSITION FROM NON-NORMAL TO NORMAL DISTRIBUTION

We observed that the distribution of Euclidean distances between randomly generated vectors tended to become normal with the increase of the vectors' dimension. Here we present the result of a finer simulation that shows the transition between non-normal and normal distribution. All the three cases (Real Positive, Real Negative and All Real) were considered and yielded equivalent results.

The simulation was performed considering vectors' dimensions spanning from $n = 2$ to $n = 12$. Kolmogorov-Smirnov tests were performed to check whether the observed simulated distribution was significantly different from a normal distribution with mean and standard deviation equal to those of the simulated data $N(\text{mean}(d), \text{std}(d))$. A p-value $p < 0.05$ was consistently observed for distributions with $n < 5$, while it presented consistently $p > 0.05$ for $n > 7$. Figure S4 presents the trend of Euclidean distance distribution for the Real Positive case in the range $2 \leq n \leq 12$. The results confirm a smooth transition between a non-normal to a normal distribution for $n > 7$.

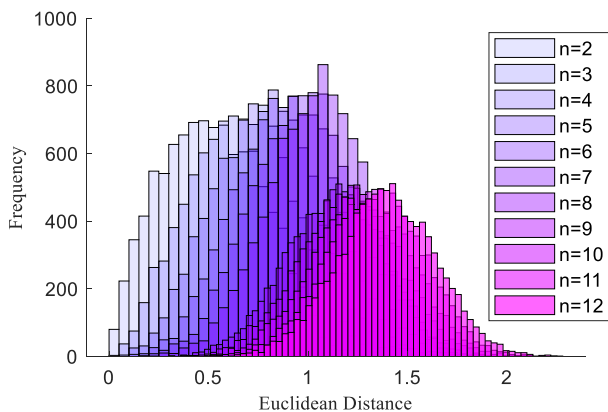


Fig. S4. Histograms of the non-normalized Euclidean distance for growing dimensions n in the range $2 \leq n \leq 12$.

ACKNOWLEDGMENT

The authors would like to thank Prof. Madhusudhan Venkadesan for his valuable feedback during the development of this manuscript.

REFERENCES

- [1] J. X. Chen, "The Evolution of Computing: AlphaGo," *Comput Sci Eng*, vol. 18, no. 4, pp. 4–7, Jul. 2016, doi: 10.1109/MCSE.2016.74.
- [2] F. Hsu, *Behind Deep Blue: Building the computer that defeated the world chess champion*. Princeton University Press, 2002. Accessed: Apr. 15, 2024. [Online]. Available: https://books.google.com/books?hl=en&lr=&id=zV0W4729UqkC&oi=fnd&pg=PR9&dq=deep+blue+chess+kasparov&ots=yrHuR4LL19&sig=GPeoCLWJtJQkfspcvri9q__c5Sc
- [3] D. Silver *et al.*, "Mastering the game of Go without human knowledge," *Nature* 2017 550:7676, vol. 550, no. 7676, pp. 354–359, Oct. 2017, doi: 10.1038/nature24270.
- [4] J. Vincent, "DeepMind's AI agents conquer human pros at StarCraft II." Accessed: Apr. 15, 2024. [Online]. Available: <https://www.theverge.com/2019/1/24/18196135/google-deepmind-ai-starcraft-2-victory>
- [5] J. Jumper *et al.*, "Highly accurate protein structure prediction with AlphaFold," *Nature* 2021 596:7873, vol. 596, no. 7873, pp. 583–589, Jul. 2021, doi: 10.1038/s41586-021-03819-2.
- [6] J. Kober, J. A. Bagnell, and J. Peters, "Reinforcement learning in robotics: A survey," *International Journal of Robotics Research*, vol. 32, no. 11, pp. 1238–1274, Sep. 2013, doi: 10.1177/0278364913495721/ASSET/IMAGES/LARGE/10.1177_0278364913495721-FIG8.JPEG.
- [7] A. M. West, F. Tessari, and N. Hogan, "The Study of Complex Manipulation via Kinematic Hand Synergies: The Effects of Data Pre-Processing," *IEEE Int Conf Rehabil Robot*, vol. 2023, pp. 1–6, Sep. 2023, doi: 10.1109/ICORR58425.2023.10304710.
- [8] J. Bennett and S. Lanning, "The Netflix Prize," 2007.
- [9] M. Santello, M. Flanders, and J. F. Soechting, "Postural Hand Synergies for Tool Use," *Journal of Neuroscience*, vol. 18, no. 23, pp. 10105–10115, Dec. 1998, doi: 10.1523/JNEUROSCI.18-23-10105.1998.
- [10] C. R. Mason, J. E. Gomez, and T. J. Ebner, "Hand Synergies During Reach-to-Grasp," *J Neurophysiol*, 2001, Accessed: Mar. 05, 2023. [Online]. Available: www.jn.org
- [11] J. Ye, "Cosine similarity measures for intuitionistic fuzzy sets and their applications," *Math Comput Model*, vol. 53, no. 1–2, pp. 91–97, Jan. 2011, doi: 10.1016/J.MCM.2010.07.022.
- [12] A. R. Lahitani, A. E. Permanasari, and N. A. Setiawan, "Cosine similarity to determine similarity measure: Study case in online essay assessment," *Proceedings of 2016 4th International Conference on Cyber and IT Service Management, CITSM 2016*, Sep. 2016, doi: 10.1109/CITSM.2016.7577578.
- [13] P. Xia, L. Zhang, and F. Li, "Learning similarity with cosine similarity ensemble," *Inf Sci (N Y)*, vol. 307, pp. 39–52, Jun. 2015, doi: 10.1016/J.INS.2015.02.024.

> REPLACE THIS LINE WITH YOUR MANUSCRIPT ID NUMBER (DOUBLE-CLICK HERE TO EDIT) <

- [14] H. V. Nguyen and L. Bai, “Cosine Similarity Metric Learning for Face Verification,” *Lecture Notes in Computer Science (including subseries Lecture Notes in Artificial Intelligence and Lecture Notes in Bioinformatics)*, vol. 6493 LNCS, no. PART 2, pp. 709–720, 2011, doi: 10.1007/978-3-642-19309-5_55.
- [15] C. Luo, J. Zhan, X. Xue, L. Wang, R. Ren, and Q. Yang, “Cosine normalization: Using cosine similarity instead of dot product in neural networks,” *Lecture Notes in Computer Science (including subseries Lecture Notes in Artificial Intelligence and Lecture Notes in Bioinformatics)*, vol. 11139 LNCS, pp. 382–391, 2018, doi: 10.1007/978-3-030-01418-6_38/FIGURES/6.
- [16] S. Eghbali and L. Tahvildari, “Fast Cosine Similarity Search in Binary Space with Angular Multi-Index Hashing,” *IEEE Trans Knowl Data Eng*, vol. 31, no. 2, pp. 329–342, Feb. 2019, doi: 10.1109/TKDE.2018.2828095.
- [17] Ö. Egecioglu, H. Ferhatosmanoglu, and U. Ogras, “Dimensionality reduction and similarity computation by inner-product approximations,” *IEEE Trans Knowl Data Eng*, vol. 16, no. 6, pp. 714–726, Jun. 2004, doi: 10.1109/TKDE.2004.9.
- [18] Y. S. Lin, J. Y. Jiang, and S. J. Lee, “A similarity measure for text classification and clustering,” *IEEE Trans Knowl Data Eng*, vol. 26, no. 7, pp. 1575–1590, 2014, doi: 10.1109/TKDE.2013.19.
- [19] J. L. W. V Jensen, “Sur les fonctions convexes et les inégalités entre les valeurs moyennes,” *Acta Mathematica*, vol. 30, no. 1, pp. 175–193, Jan. 1906, doi: 10.1007/BF02418571.
- [20] M. H. De Groot and M. J. Schervish, *Probability and Statistics*, Fourth Edition. Pearson Education, 2014.
- [21] B. Thirey and R. Hickman, “Distribution of Euclidean Distances Between Randomly Distributed Gaussian Points in n-Space,” *ArXiv*, 2015.
- [22] M. Fazle Rabbi, C. Pizzolato, D. G. Lloyd, C. P. Carty, D. Devaprakash, and L. E. Diamond, “non-negative matrix factorisation is the most appropriate method for extraction of muscle synergies in walking and running,” 2020, doi: 10.1038/s41598-020-65257-w.
- [23] M. E. Muller, “A note on a method for generating points uniformly on n-dimensional spheres,” *Commun ACM*, vol. 2, no. 4, pp. 19–20, Apr. 1959, doi: 10.1145/377939.377946.
- [24] G. Marsaglia, “Choosing a Point from the Surface of a Sphere,” <https://doi.org/10.1214/aoms/1177692644>, vol. 43, no. 2, pp. 645–646, Apr. 1972, doi: 10.1214/AOMS/1177692644.



Federico Tessari received a B.Sc. degree (cum laude) in mechanical engineering from Università degli Studi di Roma Tre in 2014, then obtained an M.Sc. degree (cum laude) in mechatronic engineering from Politecnico di Torino in 2016. In 2021, he received his Ph.D. degree (cum laude) in mechanical engineering from Politecnico di Torino together with the Italian Institute of Technology.

He is currently working as a Senior Post-Doctoral associate at the Massachusetts Institute of Technology. His research interests combine design and control of robotic and wearable devices, with the investigation of the human neuromotor control system.

Neville Hogan is Sun Jae Professor of Mechanical Engineering and Professor of Brain and Cognitive Sciences at the Massachusetts Institute of Technology. He earned a Diploma in Engineering (with distinction) from Dublin Institute of Technology and M.S., Mechanical Engineer and Ph.D. degrees from MIT. He joined MIT’s faculty in 1979 and presently directs the Newman Laboratory for Biomechanics and Human Rehabilitation. He co-founded Interactive Motion Technologies, now part of Bionik Laboratories.

His research includes robotics, motor neuroscience, and rehabilitation engineering, emphasizing the control of physical contact and dynamic interaction. Awards include: Honorary Doctorates from Delft University of Technology and Dublin Institute of Technology; the Silver Medal of the Royal Academy of Medicine in Ireland; the Saint Patrick’s Day Medal for Academia from Science Foundation Ireland; the Henry M. Paynter Outstanding Investigator Award and the Rufus T. Oldenburger Medal from the American Society of Mechanical Engineers, Dynamic Systems and Control Division; and from the Institute of Electrical and Electronics Engineers, the Academic Career Achievement Award from the Engineering in Medicine and Biology Society and the Pioneer in Robotics Award from the Robotics and Automation Society.